IEEE Access
Multidisciplinary | Rapid Review | Open Access Journal

Received June 6, 2021, accepted June 12, 2021, date of publication June 15, 2021, date of current version June 22, 2021.

Digital Object Identifier 10.1109/ACCESS.2021.3089600

Compact Dual Band Ring Coupler Using Miniaturized Metamaterial Left-Handed Impedance Inverters

IULIA ANDREEA MOCANU
Telecomunications Department, University Politehnica of Bucharest, Bucharest 060042, Romania
e-mail: iulia.mocanu@upb.ro

ABSTRACT A compact 3-dB dual band ring coupler is designed, fabricated and tested. The coupler consists of three identical miniaturized Left-Handed (LH) impedance inverter transmission lines (TLs) and a dual one. The general principle of using LH TLs' duality to reduce the size of a dual band ring coupler is explained in detail, showing the equivalent lumped element circuits and the designing relations. A numerical example is considered for the duality analysis and the results are used to obtain a size reduction for both the coupler's dimensions and the number of utilized components. Other arbitrary coupling levels (1 dB and 5 dB) and frequency ratios are investigated and the results of simulations show very good results, proving the validity of the general principle of using LH transmission line's duality. The 3-dB coupler is implemented in microstrip technology and using high-quality lumped components. It works at two arbitrary frequencies, 1.1 GHz and 2.5 GHz, respectively with similar performances. The overall dimension of the proposed coupler is $0.07\lambda \times 0.07\lambda$ for a wavelength, λ computed at 1.1 GHz. The measured results are in good agreement with the predicted ones for both frequencies, having the return loss and isolation loss better than 33 dB, whereas keeping the insertion and coupling losses at around 3.5 dB in both frequency bands. The phase imbalance at the output ports is less than 1.5°, when the difference and sum ports are excited.

INDEX TERMS Directional couplers, dual band, Left-Handed transmission lines, metamaterials, ring coupler.

I. INTRODUCTION

The demand for dual band components is increasingly high these days, as Multiple Input- Multiple Output (MIMO) components are used very often in microwave applications. An important category of microwave devices is represented by the hybrid ring couplers. They were introduced back in the 60's [1] and have been intensely studied and improved ever since. As it has been firstly proposed, this type of coupler is a monoband one using classical transmission lines acting as impedance inverters at only one central frequency, having narrow bandwidth and quite large dimensions. To transform a classical ring coupler into a dual band one, different solutions have been considered such as: artificial Composite Right Left-Handed (CRLH) transmission lines (TLs) [2]–[6], Complementary Split Ring Resonators (CSRRs) [7], substrate integrated waveguides [8], [9] or stepped impedances [10], [11]. In [3], [4], [10], [13] arbitrary power ratios have been obtained, offering more flexibility when designing a dual band ring coupler.

Also, significant efforts have been done to resume the coupler to a more compact device, suitable for the miniaturization nowadays electronics demand [12]–[15].

In this paper, all these aspects have been considered, so a general principle to design a hybrid ring coupler is presented. This principle exploits the duality of two LH transmission lines, which enables having a more compact device, working with similar performances at two arbitrary frequencies and having the possibility to achieve any arbitrary power ratios. The coupler is implemented in microstrip technology, using high-quality lumped elements.

In [2] and [4] the same technology is considered, but only one type of LH transmission lines is used. The right-handed behavior is separated from the left-handed one, which is then, implemented using lumped elements. This approach increases the bandwidth in [2] and reduces the dimension

The associate editor coordinating the review of this manuscript and approving it for publication was Qi Luo.

of the coupler in [2] and [4], but the return loss has poor results for both frequencies, only −19.62 dB and −23.39 dB, respectively. This happens mainly because the CRLH unit cells are symmetrized later in the design, not at the very beginning as in the case of the proposed coupler. Also, the coupler presented in [4] is working at a central frequency and its even harmonic, instead of two arbitrary frequencies as in this paper.

In [3] a dual band rat-race coupler is presented, implemented in microstrip technology using inclusion of two additional shunt stubs with short-circuit termination. It exhibits 39 dB for the return loss, 40.3 dB for the isolation loss, 3.3 dB and 3 dB for the insertion loss and coupling loss, respectively for the first frequency of 880 MHz. For the second frequency, 1.98 GHz, the performances are not similar: only 28.5 dB for the return loss, 29.5 dB for the isolation loss, 3.3 dB and 3.7 dB for the insertion and coupling loss, respectively. The phase imbalance for the output ports is greater than 4°. The main drawback of this coupler is the fact that it does not exhibit similar performances, especially for high frequencies.

The couplers proposed in [5] and [6] use microstrip technology, as well. The coupler in [5] can work as a branch-line coupler for a frequency band and as a ring coupler for another one. For the frequency at which it acts as a ring coupler, the measured return loss is quite poor, around 20 dB ([5], Fig. 5(a)], the isolation loss is 40 dB and the insertion and coupling losses are 3.7 dB and 3.9 dB, respectively. The phase difference at the output ports is 188.9° rather than 180° as expected. The coupler in [6] can reach any coupling levels, including 0 dB, but it works at only one frequency.

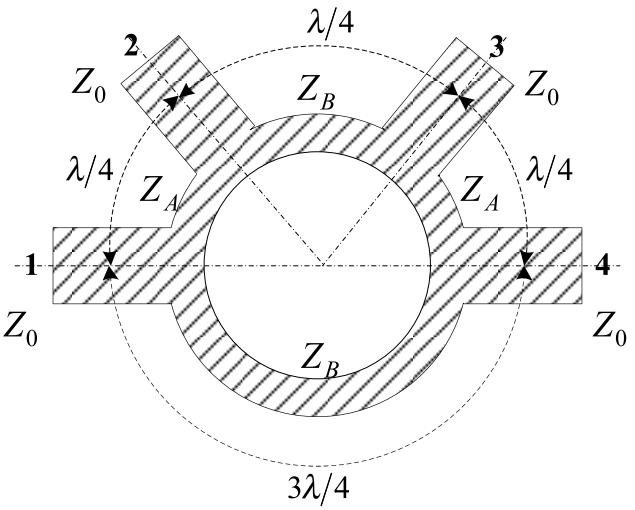

FIGURE 1. The classical, monoband ring coupler in microstrip technology.

The 3-dB coupler presented in this paper is designed starting from the classical ring coupler, depicted in Fig. 1. It is compact, miniaturized and it is working with similar performances at two arbitrary frequencies. It consists of three identical CRLH transmission lines and a dual counterpart. The design starts from the analytical expressions to compute the lumped elements of the unit cells and is then, validated using both simulations and measurements. Other levels of coupling are considered and the simulation results confirm the general principle of using duality of LH TLs. Practically, it can achieve any coupling level (except for 0 dB, as it will be demonstrated in section III of this paper) and maintain its performances.

The LH transmission lines used in this study are the CRLH and the Dual Composite Right-Left Handed (D-CRLH) ones. The CRLH TLs exhibit a right-handed behavior for certain frequencies and a left-handed behavior for other frequencies [20]. The transfer characteristic is a band-pass one and the designing frequencies must be inside this bandwidth. Another alternative with dual behavior, as the name suggests, is the classical Dual Composite Right Left-Handed (D-CRLH) transmission line [17]. The duality consists of using a parallel LC tank instead of a series one and vice versa. In this case, the transfer characteristic is a stopband one and the designing frequencies must be outside the stopband region. Another very important property is that the phases introduced by this TL are negative when compared to the positive ones of the CRLH counterpart.

II. THE ANALYSIS OF DIFFERENT TYPES OF LEFT-HANDED TRANSMISSION LINES

A. COMPOSITE RIGHT-LEFT HANDED TRANSMISSION LINES

The classical ring coupler consists of three transmission lines, with different characteristic impedances, each of length λ/4, introducing a phase shift of 90° and a different line of length 3λ/4, introducing a phase shift of 270°, at only one frequency, as shown in Fig. 1.

In Fig. 2, the principle on how to transform a classical ring coupler into a dual band one is presented. In Fig. 2(a) the monoband classical ring coupler is presented, showing only the phases introduced by each TL. Fig. 2 (b) shows how to use the phases of the Left-Handed transmission lines, including the ones having a dual band behavior. The transmission lines in the classical ring coupler, introducing a phase shift of 90° at one frequency, f_1, are replaced by transmission lines introducing a pair of phases (90°, −90°) at two arbitrary frequencies (f_1, f_2). The transmission line introducing a phase shift of 270° at the frequency f_1 is replaced either by a transmission lines introducing a pair of phases (270°, −270°) at two arbitrary frequencies (f_1, f_2) (as in [13]) or a transmission line introducing a pair of phases (−90°, 90°) at two arbitrary frequencies (f_1, f_2), as in this paper. The characteristic impedances for each transmission line remain the same as for the classical ring coupler in Fig. 1.

The promising results in [18] and [19] have demonstrated the importance of using duality, even if those studies have been carried only in the ideal case, without considering technological limitations and other levels of coupling or different frequency ratios, as in this paper.

Next, four types of LH transmission lines are analyzed comparing their performances in similar designing conditions

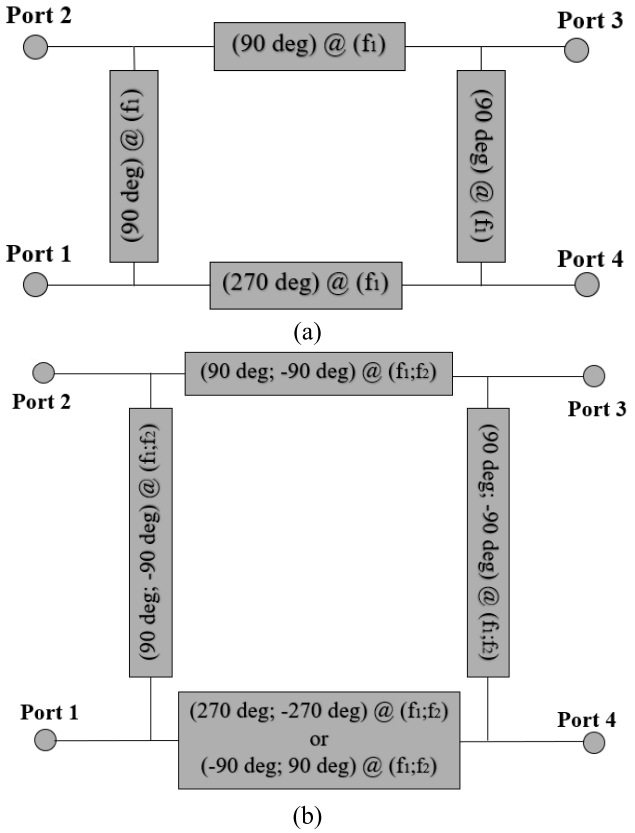

FIGURE 2. Schematic of the principle on how to use the phase shifts of TLs, keeping the characteristic impedances unchanged, to obtain a dual band ring coupler transformation: (a) TLs' phase shifts for classical monoband ring coupler, (b) LH TLs' phase shifts for dual-band ring coupler.

and conclude which is the best solution for this frequency application, keeping the ring coupler compact.

First, the classical CRLH TLs, consisting of N cascaded unit cells as defined in [16] are investigated. The CRLH unit cell is an asymmetric one made of LC lumped components. Two arbitrary frequencies: $f_1 = 1.1$ GHz and $f_2 = 2.5$ GHz and different number of cells: N = 1, 2 and 3, respectively are considered. The pair of phases introduced by the TL at two arbitrary frequencies are $\Phi_1 = 90°$, $\Phi_2 = -90°$. Other pairs of phases suggested in [16] will give negative values for the lumped elements and are not used in our study. The characteristic impedance for each transmission line in Fig. 1 is computed after imposing the coupling attenuation, $A_C = 3$ dB and the reference impedance $Z_0 = 50\ \Omega$ [1]:

$$C = 10^{-A_c/10}, \quad Z_A = \frac{Z_o}{\sqrt{1-C}}, \; Z_B = \frac{Z_o}{\sqrt{C}} \tag{1}$$

For a hybrid ring coupler, using relations (1), the characteristic impedances are $Z_A = Z_B = Z_C = 70.71\ \Omega$. The analytical relations used to determine the values for the lumped components modeling the Right-Handed (index R) and Left-Handed (index L) effects and the cut-off frequencies are the ones given in [17]:

$$L_R = \frac{Z_C\left[\Phi_1 \cdot (f_1/f_2) - \Phi_2\right]}{N \cdot 2 \cdot \pi \cdot f_2\left[1 - (f_1/f_2)^2\right]}, \tag{2a}$$

$$C_R = \frac{\Phi_1 \cdot (f_1/f_2) - \Phi_2}{N \cdot 2 \cdot \pi \cdot f_2 \cdot Z_C\left[1 - (f_1/f_2)^2\right]}, \tag{2b}$$

$$L_L = \frac{N \cdot Z_C\left[1 - (f_1/f_2)^2\right]}{2 \cdot \pi \cdot f_1\left[\Phi_1\,(f_1/f_2) - \Phi_2\right]}, \tag{2c}$$

$$C_L = \frac{N\left[1 - (f_1/f_2)^2\right]}{2 \cdot \pi \cdot f_1 \cdot Z_C\left[\Phi_1\,(f_1/f_2) - \Phi_2\right]}, \tag{2d}$$

$$f_{c_{L,R}} = \frac{1}{2\pi\sqrt{L_R C_R}}\left|1 \mp \sqrt{1 + \sqrt{\frac{L_R C_R}{L_L C_L}}}\right|. \tag{2e}$$

The two arbitrary frequencies must be in the bandpass defined by the two cut-off frequencies, f_{cL} and f_{cR}, for the TL to be used. This condition is fulfilled for 2, 3 or a higher number of cells. To minimize the structure, but still have the desired performances, two cells are further considered for investigation. The next step is to transform the asymmetric unit cells into symmetric ones to improve the frequency response, as demonstrated in [17]. The type of symmetry is not important, so a "T" is chosen. The two-unit cells CRLH TL equivalent circuit is depicted in Fig. 3 (a).

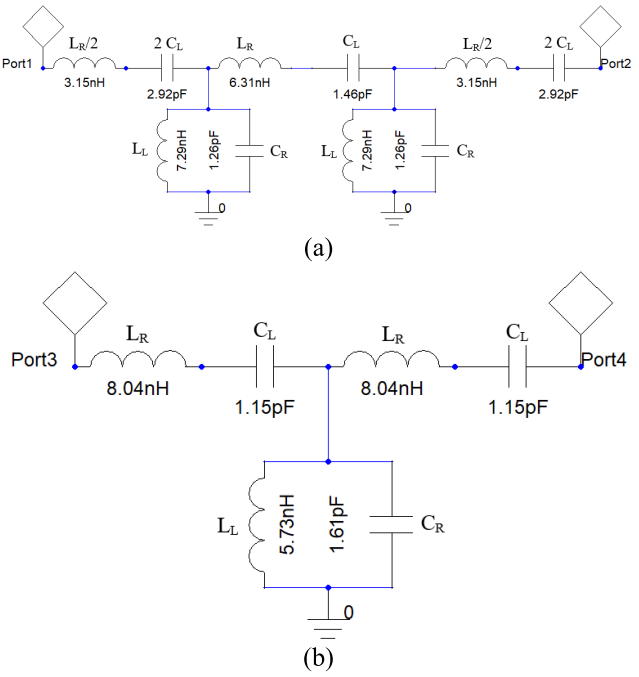

FIGURE 3. (a) Schematic of the CRLH TL with two cells. (b) Schematic of the single cell CRLH TL impedance inverter.

The other type of CRLH TL investigated is the one proposed by the author in [18]. The advantages of this type of CRLH impedance inverter TL are the fact that the unit cell is already symmetrized, the number of cells is minimum to assure sufficient bandpass for the two arbitrary frequencies to fit in and the frequency behavior is of a dual

band impedance inverter. To obtain this type of unit cell, the circuit with normalized immittances has been introduced in [18]. Then, choosing an arbitrary characteristic impedance, they have been de-normalized. When de-normalizing, for a CRLH unit cell to be obtained, in the longitudinal branches, a capacitor in series with an inductor must be placed, whereas in the transversal branch, a capacitor in parallel with an inductor must be put. For a D-CRLH unit cell, a capacitor in parallel with an inductor are placed in the longitudinal branch, whereas in the transversal branch, a capacitor in series with an inductor is put. These types of unit cells fulfill the classical matching condition for CRLH transmission lines: $L_R C_L = L_L C_R$, so they have a characteristic impedance frequency independent [16]. For designing this type of CRLH TL, the analytical relations demonstrated in [18] are used:

$$L_R = \frac{1}{f_2 - f_1} \cdot \frac{Z_c}{2 \cdot \pi}, \tag{3a}$$

$$C_L = \frac{f_2 - f_1}{2 \cdot \pi \cdot f_1 \cdot f_2 \cdot Z_C}, \tag{3b}$$

$$C_R = \frac{1}{f_2 - f_1} \cdot \frac{1}{2 \cdot \pi \cdot Z_c}, \tag{3c}$$

$$L_L = \frac{f_2 - f_1}{f_1 \cdot f_2} \cdot \frac{Z_c}{2 \cdot \pi}. \tag{3d}$$

With the imposed values for the frequencies and the characteristic impedance, Z_C the values for the lumped elements of the unit cell are: $L_L = 5.73$ nH, $C_L = 1.15$ pF, $L_R = 8.04$ nH, $C_R = 1.61$ pF. This alternative one-cell CRLH TL is depicted in Fig. 3.(b). The simulation results for both types of CRLH TLs are given in Fig. 4 for the return loss, in Fig. 5 for the insertion loss and in Fig. 6 for the phase difference.

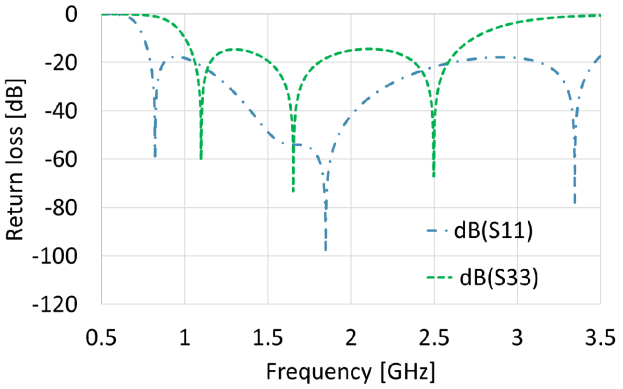

FIGURE 4. Return loss for the transmission line in Fig. 3a) -dB(S_{11}) and return loss for transmission line in Fig. 3b) -dB(S_{33}).

As observed from Fig. 4, the return loss for the classical CRLH transmission line is around 21 dB rather than 66 dB for the one unit-cell impedance inverter TL, at both frequencies. On the other hand, Fig. 5 shows a constant, almost 0dB insertion loss in the bandpass for the CRLH TL in Fig. 3a) rather than the one with ripples in the case of the line in Fig3.b). On the other hand, the appearance of the ripples does not affect the value of the insertion loss at the designing

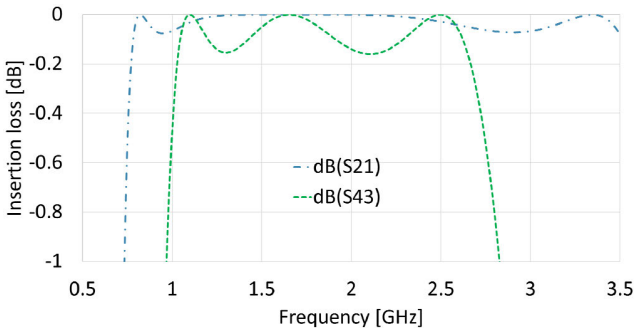

FIGURE 5. Insertion loss for the transmission line in Fig. 3a) -dB(S_{21}) and insertion loss for transmission line in Fig. 3b) -dB(S_{43}).

TABLE 1. Return loss, insertion loss and phase difference for different CRLH TLs.

Parameter	Type of CRLH TL	f_1 [GHz]	f_2 [GHz]
Return loss [dB]	2-cell CRLH TL	21.32	21.88
	1-cell CRLH TL	60.07	66.83
Insertion loss [dB]	2-cell CRLH TL	0.03	0.03
	1-cell CRLH TL	0	0
Phase difference [deg]	2-cell CRLH TL	93.06	-91.88
	1-cell CRLH TL	90.08	-89.98

frequency. Due to the increased number of cells for the line in Fig. 3a), the bandpass is larger than in the case of one-unit cell transmission line. Still, the insertion loss required for the two working frequencies is 0.03 dB for the one-cell transmission line. Also, for the one-cell transmission line, the phase difference is almost equal to $\pm 90°$ rather than 93°, respectively $-91.88°$ for the classical CRLH TL. The synthesized results in Table 1 confirm that the alternative impedance inverter TL exhibits significantly improved performances at both frequencies, when compared to classical CRLH transmission lines. These types of structures are extremely sensitive to approximations, so symmetrizing them afterwards will lead to poorer results.

B. DUAL COMPOSITE RIGHT LEFT-HANDED TRANSMISSION LINES

The next step is to replace the $3\lambda/4$ monoband transmission line in Fig. 1 (a) with a dual band transmission line as presented in Fig. 2 (b). One way suggested in literature [2] is to use CRLH transmission lines designed to introduce a pair of phases $\Phi_1 = 270°$, $\Phi_2 = -270°$ at the two arbitrary frequencies. This means using a classical CRLH TL, but this time imposing the needed pair of phases. The values for the lumped components and the two cut-off frequencies are determined by imposing a number of 1, 2 and 3 cells, respectively. Then, the analytical expressions from (2) are used. A minimum number of three cells is required to create a CRLH TL for which both working frequencies are in the band-pass. This means an even higher number of elements

than in the previous case. This approach leads to a more complex structure, with increased losses and parasitic effects, when implemented using real components. So, next the duality of the D-CRLH transmission lines [17] is analyzed.

The relations used for computing both the lumped elements modeling the Right-Handed (index R) and Left-Handed (index L) effects and the cut-off frequencies for a classical D-CRLH line, are the ones demonstrated in [20]:

$$L_R = \frac{Z_c \cdot \Phi_1 \cdot \Phi_2 \left[1 - (f_1/f_2)^2\right]}{N \cdot 2 \cdot \pi \cdot f_1 \left[\Phi_2 - \Phi_1 \cdot (f_1/f_2)\right]}, \tag{4a}$$

$$L_L = \frac{N \cdot Z_c \cdot \left[(f_1/f_2) \cdot \Phi_2 - \Phi_1\right]}{2 \cdot \pi \cdot f_2 \cdot \Phi_1 \cdot \Phi_2 \left[1 - (f_1/f_2)^2\right]}, \tag{4b}$$

$$C_R = \frac{\Phi_1 \cdot \Phi_2 \left[1 - (f_1/f_2)^2\right]}{N \cdot Z_c \cdot 2 \cdot \pi \cdot f_1 \left[\Phi_2 - \Phi_1 \cdot (f_1/f_2)\right]}, \tag{4c}$$

$$C_L = \frac{N \cdot \left[(f_1/f_2) \cdot \Phi_2 - \Phi_1\right]}{Z_c \cdot 2 \cdot \pi \cdot f_2 \cdot \Phi_1 \cdot \Phi_2 \left[1 - (f_1/f_2)^2\right]}. \tag{4d}$$

$$f_{cL,R} = \frac{(2\pi)^{-1}}{\sqrt{L_R C_L}} \times \sqrt{1 + \frac{\sqrt{L_R C_R}}{8\sqrt{L_L C_L}} \pm \sqrt{\frac{\sqrt{L_R C_R}}{4\sqrt{L_L C_L}}} \sqrt{1 + \frac{\sqrt{L_R C_R}}{16\sqrt{L_L C_L}}}} \tag{4e}$$

A number of unit cells, N = 1, 2 and 3, respectively is imposed. After computations, it can be observed that two cells are enough to assure that both working frequencies are outside the stopband given by the two cut-off frequencies. The values for the lumped components of the unit cell, imposing the value for the characteristic impedance $Z_C = 70.71\ \Omega$, are: $L_R = 4.5$ nH, $C_R = 0.9$ pF, $L_L = 10.2$ nH, $C_L = 2.04$ pF and the equivalent circuit is presented in Fig. 7(a).

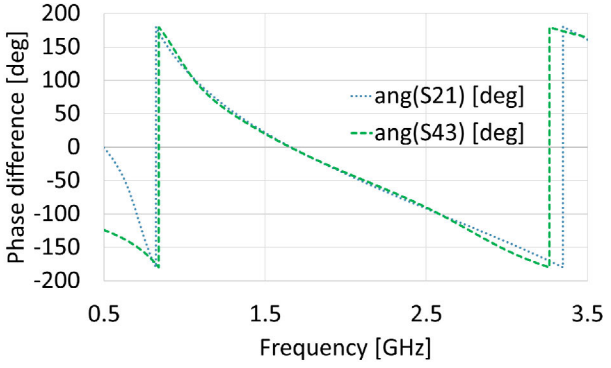

FIGURE 6. Phase difference for the transmission line in Fig. 3a) -ang(S_{21}) and phase difference for transmission line in Fig. 3b) -ang(S_{43}).

So, just by using a different approach, as depicted in Fig. 2(b), a two-cell LH transmission line can be used instead of a three-cell one.

Next, the one-unit cell D-CRLH impedance inverter from [18] is inspected. The values for the lumped components

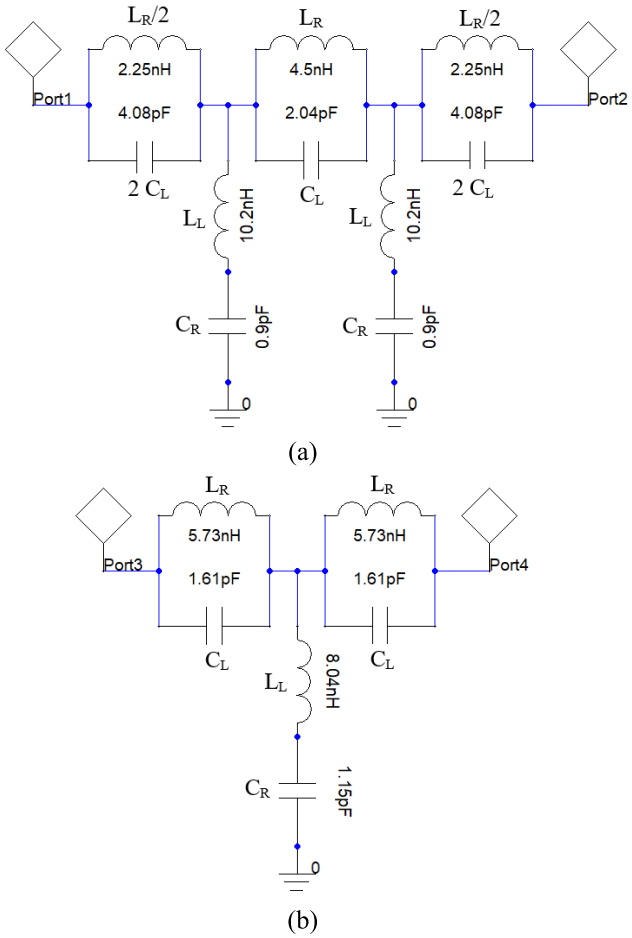

FIGURE 7. (a) Schematic of the D-CRLH TL with two cells. (b) Schematic of the single cell D-CRLH TL impedance inverter.

are computed using relations demonstrated in [18]:

$$L_L = \frac{1}{f_2 - f_1} \cdot \frac{Z_c}{2 \cdot \pi}, \tag{5a}$$

$$C_R = \frac{f_2 - f_1}{2 \cdot \pi \cdot f_1 \cdot f_2 \cdot Z_C}, \tag{5b}$$

$$C_L = \frac{1}{f_2 - f_1} \cdot \frac{1}{2 \cdot \pi \cdot Z_c}, \tag{5c}$$

$$L_R = \frac{f_2 - f_1}{f_1 \cdot f_2} \cdot \frac{Z_c}{2 \cdot \pi} \tag{5d}$$

With the imposed values for the frequencies and the characteristic impedance, Z_C the values for the lumped elements are determined: $L_R = 5.73$ nH, $C_R = 1.15$ pF, $L_L = 8.04$ nH, $C_L = 1.61$ pF. This design guarantees that the working frequencies are outside the band stop, so no cut-off frequencies are defined or used as in [20]. The lumped elements circuit is given in Fig. 7 (b).

The results of the simulations for the transmission lines in Fig. 7 (a) and Fig. 7 (b) are given in Fig. 8 for the return loss, in Fig. 9 for the insertion loss and in Fig. 10 for the phase difference.

The return loss in the case of one-unit cell D-CRLH impedance inverter is 67.45 dB for the first frequency and

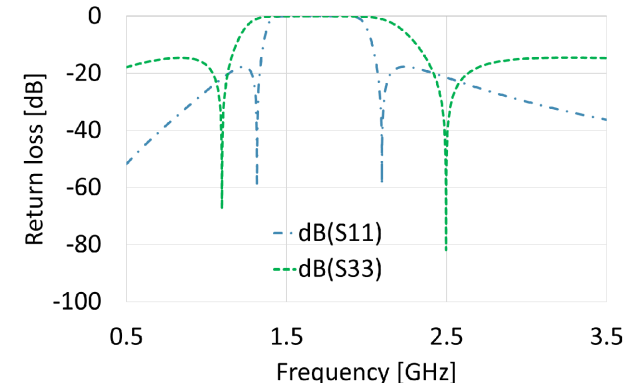

FIGURE 8. Return loss for the transmission line in Fig. 7 (a) -dB(S_{11}) and return loss for the transmission line in Fig. 7 (b) -dB(S_{33}).

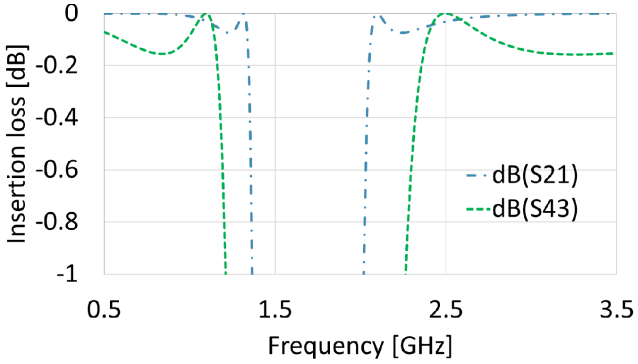

FIGURE 9. Insertion loss for the transmission line in Fig. 7 (a) -dB(S_{21}) and insertion loss for transmission line in Fig. 7 (b) -dB(S_{43}).

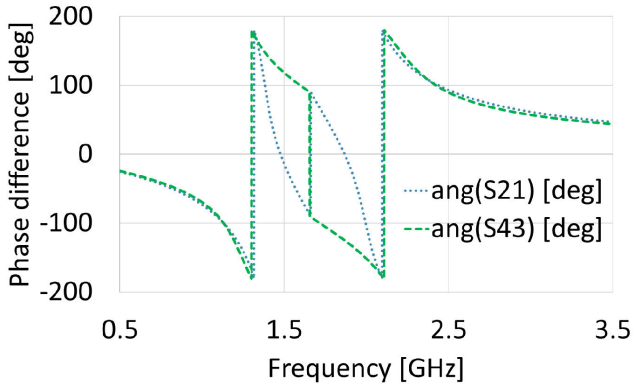

FIGURE 10. Phase difference for the transmission line in Fig. 7 (a) -ang(S_{21}) and phase difference for transmission line in Fig. 7 (b) -ang(S_{43}).

81.84 dB for the second one. The classical D-CRLH TL containing two cells has a return loss of only 21.75 dB, respectively 21.4 dB. The insertion losses are almost equal to 0 dB for both types of transmission lines and the phase differences are showing the dual behavior of this lines compared to CRLH lines. For the one-unit cell D-CRLH, the phase difference is $-90.19°$, respectively $90.02°$ rather than $-92°$, respectively $93.38°$. The advantages of using one-cell D-CRLH impedance inverters are obvious when observing the performances and the number of components required to implement it.

TABLE 2. Return loss, insertion loss and phase difference for different D-CRLH TLs.

Parameter	Type of D-CRLH TL	f_1 [GHz]	f_2 [GHz]
Return loss [dB]	2-cell D-CRLH TL	21.75	21.4
	1-cell D-CRLH TL	67.45	81.84
Insertion loss [dB]	2-cell D-CRLH TL	0.03	0.03
	1-cell D-CRLH TL	0	0
Phase difference [deg]	2-cell D-CRLH TL	-92	93.38
	1-cell D-CRLH TL	-90.19	90.02

The results obtained after simulation for both D-CRLH TLs are synthesized in Table 2.

Comparing the results after simulations for all four types of artificial transmission lines, the alternative CRLH and D-CRLH impedance inverters transmission lines are best suited for this application, as they have the minimum number of components and improved performances, due to their symmetrized design.

C. PERFORMANCES OF CRLH AND D-CRLH TRANSMISSION LINES FOR DIFFERENT FREQUENCY RATIOS

Different frequency ratios are considered to determine if the results obtained previously are still valid. The frequency ratio analyzed in previous sections A and B is equal to 2.27. Other two pair of frequencies are imposed, resulting different frequency ratios: $f_1 = 1.1$ GHz and $f_2 = 1.54$ GHz ($f_2/f_1 = 1.4 < 2.27$), respectively $f_1 = 1.1$ GHz and $f_2 = 4.1$ GHz ($f_2/f_1 = 3.727 > 2.27$). The TLs are considered ideal and the values for the lumped elements and cut-off frequencies (f_{cR} and f_{cL}) are computed using relations (2)-(5). For the 2-cell CRLH TL, the cut-off frequencies are 0.85 GHz and 1.97 GHz, corresponding to the first pair of frequencies and 0.55 GHz and 8.19 GHz, corresponding for the second pair of frequencies. For the 2-cell D-CRLH transmission line, the cut-off frequencies are 1.21 GHz and 1.39 GHz, corresponding to the first pair of frequencies and 1.61 GHz and 2.79 GHz, corresponding to the second one. The simulation results for the return loss, insertion loss and phase difference are presented in Table 3 and Table 4.

Analyzing the results in Table 3 and 4, it can be observed that the return loss is significantly improved for the case of one-cell CRLH and one-cell D-CRLH TLs. The return loss for one-cell CRLH TL is better than 51.76 dB rather than 21.4 dB for the classical 2-cell CRLH TL, in both cases. For the one-cell D-CRLH TL, the return loss has values greater than 73.82 dB rather than only 11.8 dB in the case of the two-cells D-CRLH TLs. The explanation is that the classical, two-cell CRLH and D-CRLH TLs work in a certain bandwidth imposed by the cut-off frequencies. When the designing frequencies are close to the cut-off frequencies, the performances become poor. This can be

TABLE 3. Return loss, insertion loss and phase difference for different CRLH TLs at different frequencies.

Frequency [GHz]	Type of CRLH TL	Return loss [dB]	Insertion loss [dB]	Phase difference [deg]
1.1	2-cell TL	21.4	0.03	93.08
	1-cell TL	51.76	0	90.16
1.54	2-cell TL	21.71	0.03	-92.04
	1-cell TL	55.47	0	-89.87
1.1	2-cell TL	21.57	0.03	92.5
	1-cell TL	77.23	0	90.02
4.1	2-cell TL	21.6	0.03	-92.49
	1-cell TL	82.85	0	-90.02

TABLE 4. Return loss, insertion loss and phase difference for different D-CRLH TLs at different frequencies.

Frequency [GHz]	Type of D-CRLH TL	Return loss [dB]	Insertion loss [dB]	Phase difference [deg]
1.1	2-cell TL	19.15	0	107.95
	1-cell TL	89.62	0.05	-90.46
1.54	2-cell TL	11.8	0.3	73.91
	1-cell TL	95.52	0	90.13
1.1	2-cell TL	21.57	0.03	-92.48
	1-cell TL	73.82	0	-89.98
4.1	2-cell TL	21.57	0.03	92.48
	1-cell TL	81.66	0	90.03

observed especially in the case of the pair of frequencies $f_1 = 1.1$ GHz and $f_2 = 1.54$ GHz for the D-CRLH 2-cell TL, which has the cut-off frequencies $f_{cL} = 1.218$ GHz and $f_{cR} = 1.391$ GHz. This fact also affects the phase difference, which is 107.95° for the first frequency and 73.91° for the second frequency rather than −90°/90°. The one-cell impedance inverters TLs do not require computing a cut-off frequency, so the performances will always be very good at the designing frequencies. Moreover, the fact that these unit cells are already symmetrized provide values for the phase difference very close to ideal ones. So, the one-cell CRLH and D-CRLH transmission lines can be used successfully for any kind of frequency ratios.

III. THE ANALYSIS OF DIFFERENT COUPLING LEVELS

The one-cell CRLH/D-CRLH impedance inverters have proven better performances than the classical ones, when imposing a 3 dB coupling attenuation and different frequency ratios. Further on, different coupling levels are considered and the performances of the ring coupler using these TLs are investigated. As seen in relations (1), the coupling level influences only the values of the characteristic impedances. The principle described in Fig. 2 remains valid no matter what coupling level is chosen. The only limitation is about a coupling loss of 0 dB, which is impossible to achieve, as it leads to an infinity value for the characteristic impedance. Other arbitrary coupling levels can be chosen, so for further investigation a coupling level of $A_C = 1$ dB and 5 dB, respectively are imposed. For a coupling loss of 1 dB, the characteristic impedances are $Z_A = 110.25\ \Omega$ and $Z_B = 56.1\ \Omega$. For the 5 dB coupling loss, the characteristic impedances are $Z_A = 60.466\ \Omega$ and $Z_B = 88.91\ \Omega$. These values are then introduced in relations (3a)-(3d) and (5a)-(5d), respectively and the CRLH/D-CRLH impedance inverters TLs are designed for each case. Using these lines, the ring couplers are created. The simulation frequency response of the ideal 1-dB and 5-dB dual band ring couplers are given in Fig. 11 (a) and Fig. 12 (a) for the transfer parameters and in Fig. 11 (b) and Fig. 12 (b) for the phase difference with the difference and sum ports excited-ang(S_{21})-ang(S_{41}), respectively ang(S_{12})-ang(S_{32}).

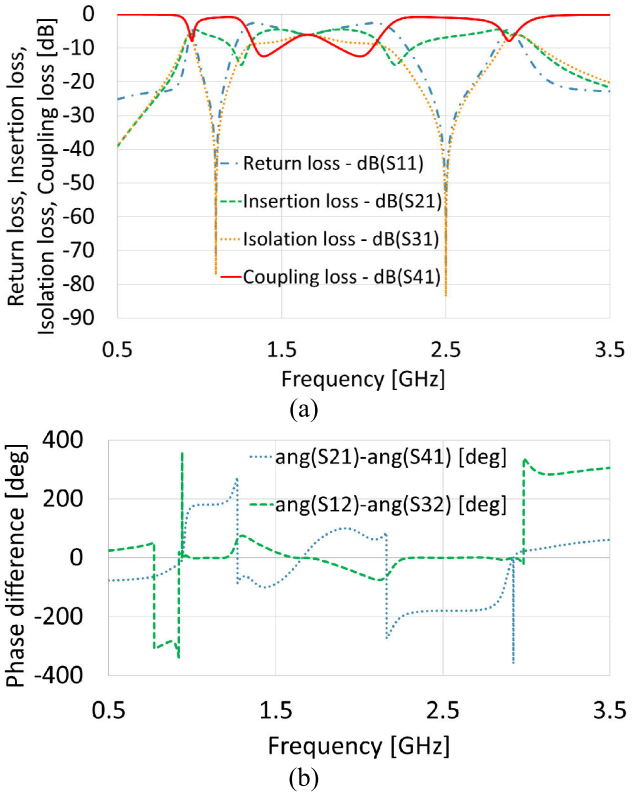

FIGURE 11. Simulation frequency response for the ideal 1-dB ring coupler. (a) Return loss -dB(S_{11}), insertion loss -dB(S_{21}), isolation loss -dB(S_{31}), coupling loss -dB(S_{41}), port 1 being the excited port. (b) Output phase difference with the difference and sum ports excited-ang(S_{21})-ang(S_{41}), respectively ang(S_{12})-ang(S_{32}).

The return loss – dB(S_{11}) and the isolation loss -dB(S_{31}) are better than 75 dB at both frequencies, for 1-dB and 5-dB coupling levels. These values are obtained for the ideal case, not considering the effect of losses and approximations introduced by the standardized values for the lumped components, as it will be detailed in Section IV of this paper. The coupling losses are exactly as the ones imposed by the design: 1 dB, respectively 5 dB. The phase difference, ang(S_{21})-ang(S_{41}) is ±180° and the phase difference, ang(S_{12})-ang(S_{32}) is 0°

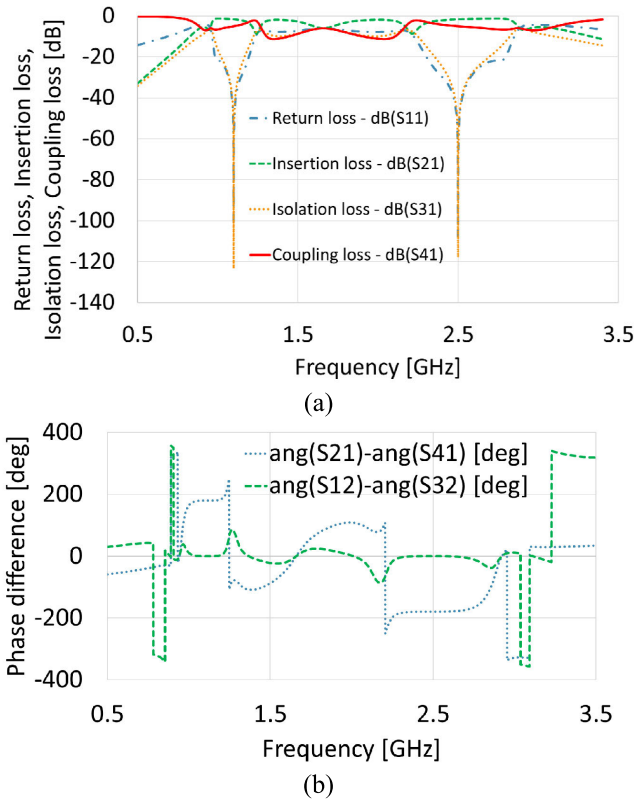

FIGURE 12. Frequency response for the ideal 5-dB ring coupler. (a) Return loss –dB(S_{11}), insertion loss -dB(S_{21}), isolation loss -dB(S_{31}), coupling loss -dB(S_{41}), port 1 being the excited port. (b) Output phase difference with the difference and sum ports excited ang(S_{21})-ang(S_{41}), respectively ang(S_{12})-ang(S_{32}).

at both frequencies, in both cases, when port 1, respectively port 2 are excited.

The 15-dB return loss bandwidth of S_{11} with the coupling loss 1 dB is 16.36% (1-1.18 GHz), respectively 16.4% (2.33-2.73 GHz) at 1.1 GHz and 2.5 GHz. For the coupling loss of 5 dB, the bandwidth is 21.8% (0.97-1.21 GHz) and 22.4% (2.26-2.82 dB) respectively. These values are better than the ones reported in [5], where the bandwidth is 16 %. The results of the simulation in the ideal case indicates that the design is correct, no matter the imposed value for the coupling levels.

IV. MINIATURIZED DUAL BAND RING COUPLER

Once the LH transmission lines have been selected for the ring coupler's construction, real lumped components need to be chosen. The utilized components are AVX Accu-L 0603 chip capsules for inductors and AVX Accu-P 0603 chip capsules for capacitors. They were considered for having tight tolerances and high-quality factor, being recommended by the producer for microwave applications, which require miniaturization and increasing frequencies. Because the standardized available components do not have the exact values resulted from computations, a fine-tuning is required. When tuning, a compromise over the performances achieved at both frequencies must be considered. No series or parallel combinations are used as in [2] and [19], keeping the number of lumped elements to a minimum, as desired by the design.

TABLE 5. Standardized available lumped elements for CRLH and D-CRLH TLs.

	Symbol	Ideal	Standardized
Lumped components	Ll	5.73 nH	5.6 nH
	Lr	8.04 nH	8.2 nH
	Cr	1.61 pF	1.6 pF
	Cl	1.15 pF	1.1 pF

The final standardized values for the lumped elements used to create the unit cells for both CRLH and D-CRLH transmission lines are given in Table 5.

The substrate used is Arlon CuClad 250 ($\varepsilon_r = 2.5$, $\tan\delta = 0.0018$) with a thickness of 0.254 mm and Cooper metallization with a thickness of 18 um. The substrate offers stable dielectric constant over a wide frequency range and low circuit losses at high frequency, being recommended for microwave applications such as filters and couplers, as the producer suggests. Having defined the characteristics of the substrate and the standardized values for the lumped components, the pads for the lumped components are added in the design. The width of the access transmission line is 0.9 mm to have a 50 Ω matching. The SMA (SubMiniature version A) connecters are mounted on the structure using mechanical welding.

The SMA has a 50 Ω characteristic impedance and is designed to work in the range 0–18 GHz.

The schematic and the fabricated miniaturized ring coupler prototype are given in Fig. 13. The overall dimension of the coupler including the access lines is $0.07\lambda \times 0.07\lambda$, where the wavelength λ is computed at the frequency f_1, considering the relative permittivity of the dielectric. The dimension of the coupler is 1.8 times smaller than the one reported in [2].

The metamaterial character of the LH transmission lines is provided by their characteristics detailed in sections A and B and by their dimensions: each CRLH and D-CRLH transmission line has a length of 9 mm, which represents a length of approximately λ/20.

The ring coupler has been connected to the Agilent E5071C (9 kHz to 6.5 GHz) network analyzer through 50 Ω cables. A short-open-load-through (SOLT) calibration was performed using the Agilent calibration Kit, before starting the measurements. The number of sweep points is chosen 1601.

The results are given in Fig. 14 for the simulated and measured return loss -dB(S_{11}) and isolation loss- S_{31}, in Fig. 15 for the simulated and measured insertion loss -dB(S_{21}) and coupling loss -dB(S_{31}), in Fig. 16 for the simulated and measured output phase difference- ang(S_{21})-ang(S_{41}) when the difference port, port 1 is excited, in Fig 17 for the simulated and measured output phase

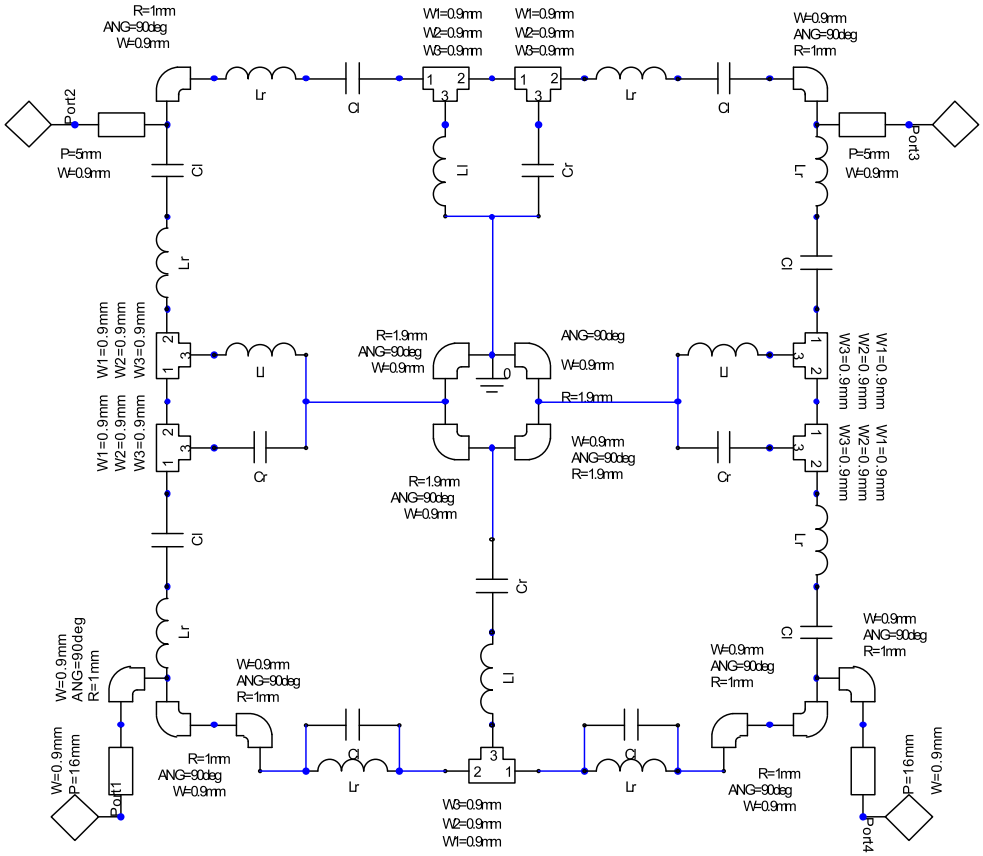

(a)

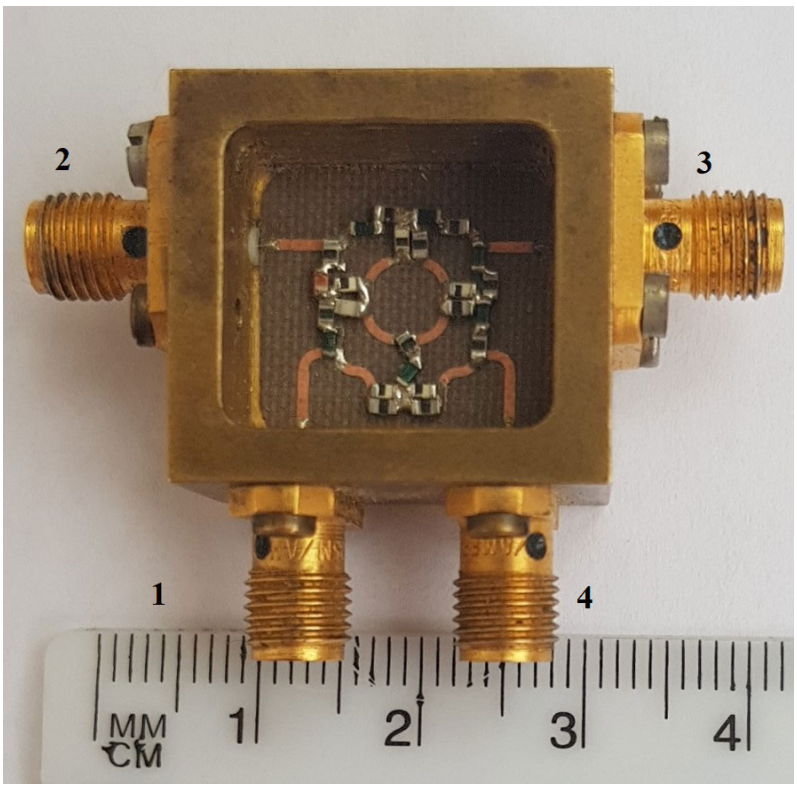

(b)

FIGURE 13. The miniaturized dual band ring coupler: (a) Schematic of the proposed coupler, (b) Fabricated prototype.

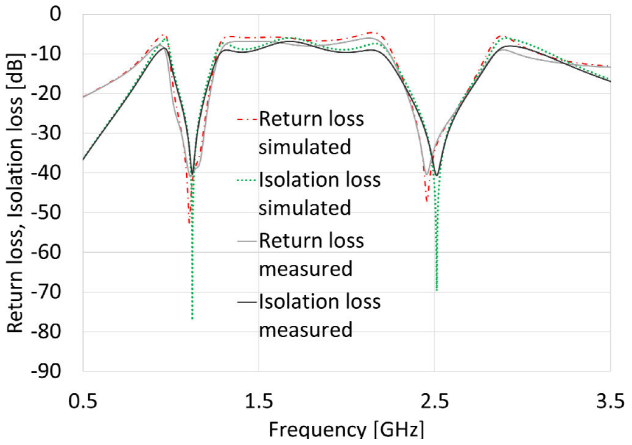

FIGURE 14. Simulated and measured return loss- dB(S_{11}) and isolation loss -dB(S_{41}).

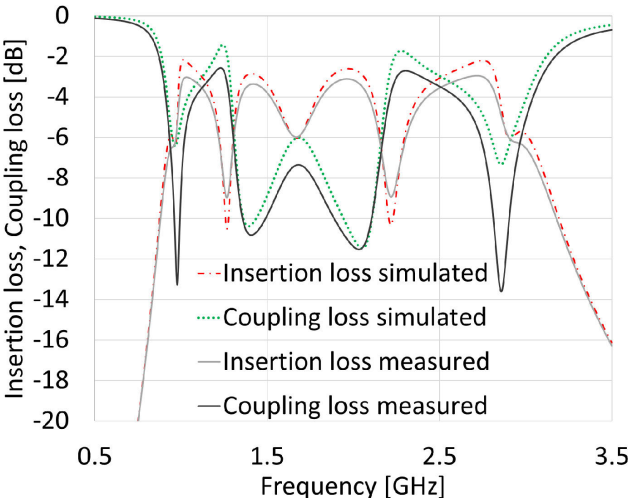

FIGURE 15. Simulated and measured insertion loss- dB(S_{21}) and coupling loss- dB(S_{41}).

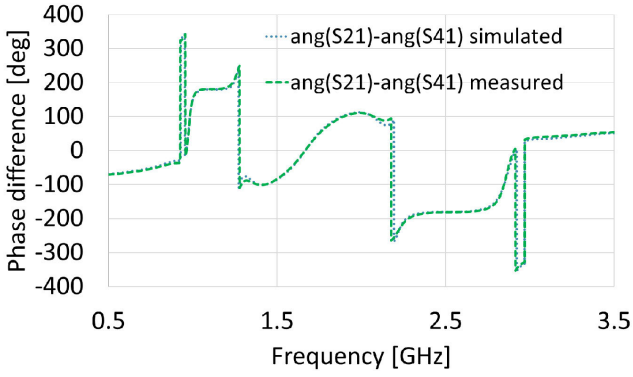

FIGURE 16. Simulated and measured output phase difference- ang(S_{21})-ang(S_{41}), when the difference port, port 1 is excited.

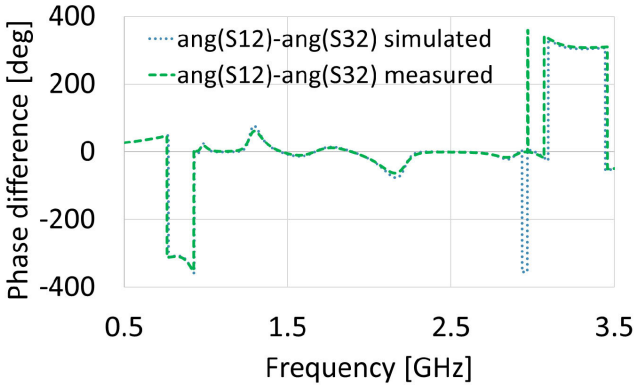

FIGURE 17. Simulated and measured output phase difference- ang(S_{12})-ang(S_{32}), when the sum port, port 2 is excited.

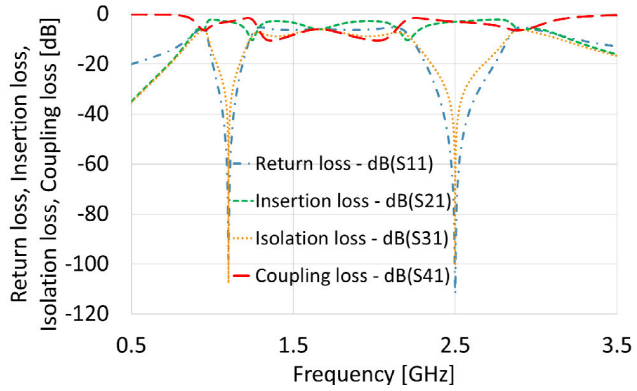

FIGURE 18. Return loss- dB(S_{11}), insertion loss – dB(S_{21}), insolation loss – dB(S_{31}), coupling loss- dB(S_{41}) for the ideal schematic lumped circuit of the final proposed dual-band coupler structure.

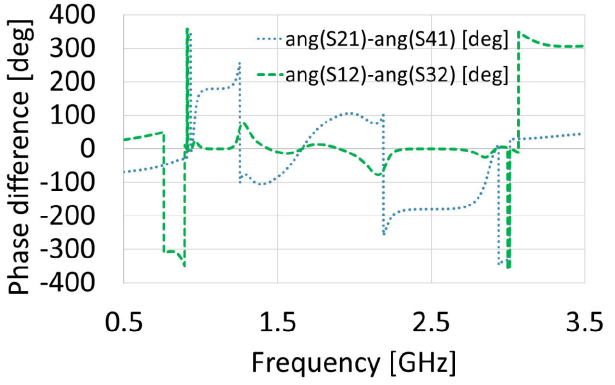

FIGURE 19. Output phase difference for the ideal schematic lumped circuit of the final proposed dual-band coupler structure, when the difference port, port 1 and the sum port, port 2 are excited, respectively.

difference- ang(S_{12})-ang(S_{32}), when the sum port, port 2 is excited.

In Fig. 18 and 19, there are given the schematic lumped circuit results of the final proposed dual-band coupler structure, which represent the ideal case. When comparing these results, there can be noticed a slight frequency shift for the value of the return loss because of using standardized values for the lumped elements and not being capable to perfectly compensate the phase shifts introduced by the interconnection transmission lines.

The effect of losses introduced by a finite, frequency dependent quality factor of the lumped components, especially for inductors, can be seen affecting mostly the results in Fig. 14 and Fig. 15, meaning the transfer parameters, when compared to the results in Fig. 18.

TABLE 6. Results of the simulated and measured parameters characterizing the proposed ring coupler.

Parameters	Simulated		Measured		Schematic lumped circuit	
	1.1 [GHz]	2.5 [GHz]	1.1 [GHz]	2.5 [GHz]	1.1 [GHz]	2.5 [GHz]
Return loss [dB]	52.52	40.32	41	33.64	98	111.96
Isolation loss [dB]	55.49	62.02	33.14	38.8	107.73	100.64
Insertion loss [dB]	2.93	3.03	3.47	3.52	3.01	3.01
Coupling loss [dB]	3.15	2.96	3.44	3.57	3.01	3.01
Output phase difference – ang(S_{21})-ang(S_{41}) [deg]	180.08	-180.05	181.1	-181.4	180	-180
Output phase difference – ang(S_{12})-ang(S_{32}) [deg]	-0.08	0.1	1.18	-1.04	0	0

The results for the main parameters of the coupler, both simulated and measured, respectively the schematic lumped circuit results of the final proposed dual-band coupler structure at the frequencies of 1.1 GHz and 2.5 GHz are synthesized in Table 6. It can be observed that the less affected by the losses and approximations are the values for the output phase difference. There is less than 2° phase difference between he measured and the ideal results. This happens mainly because the artificial transmission lines used to implement the coupler are impedance inverter types.

A comparison with the performances of other dual-band ring couplers in literature is given in Table 7.

For the proposed coupler, a return loss of 41 dB at 1.1 GHz and 33.64 dB at 2.5 GHz have been measured. The coupler presented in [2] is working at two arbitrary frequencies and is implemented in microstrip technology and using lumped elements. The return loss is 19.62 dB at 2.4 GHz and 23.39 dB at 5.2 GHz. The coupler in [3], implemented using only microstrip technology, exhibits improved results (39 dB at 0.88 GHz and 28.5 dB at 1.98 GHz), but not as good as in the case of the proposed coupler. In [5], a dual mode coupler is presented, designed to act as a branch-line coupler at 1.5 GHz and as a rat-race coupler at 2.5 GHz. The technology used for implementation is similar to the one proposed in this paper: microstrip and lumped elements. The return loss for the rat-race coupler, measured at 2.5 GHz is less than 25 dB ([5], Fig. 5(a)].

The measured isolation loss for the proposed coupler is 33.14 dB for the first frequency and 38.8 dB for the second one. In [5] the isolation loss is 40 dB at 2.5 GHz, whereas in [2] it is 29.97 dB for 2.4 GHz and 22.11 dB for 5.2 GHz. In [3], the isolation loss has slightly higher values for the first frequency (40.3 dB at 0.88 GHz), but smaller for the second one (29.5 dB at 1.98 GHz).

The measured insertion and coupling losses are around 3.45 dB for 1.1 GHz and 3.55 dB for the 2.5 GHz. In [2] the reported values for the insertion and coupling losses are poorer (around 4 dB) than in the case of the proposed coupler. In [3] the insertion and coupling losses are around 3.3 dB, as the technology does not involve using lumped elements. In [5] the measured insertion and coupling losses are 3.7 dB and 3.9 dB at 2.5 GHz, so approximately similar results are obtained.

For the proposed coupler, the phase imbalance is around ±1°, when the difference and sum ports are excited. In fact, these parameters are less influenced by losses than the transfer parameters.

In [2], the reported values are 4.3° at 2.4 GHz and 1.9° at 5.2 GHz, whereas in [3] the output phase difference is 184.6° and 177.8°, when the difference port is excited and 5.1° and 4.9°, when the sum port is excited. In [5], the measured output phase differences are 5.5° and 188.8° respectively, when the sum and difference ports are excited, so the phase imbalance is higher than in the case of the proposed coupler. So, in the case of the proposed coupler, very good results for the output phase difference have been obtained. The measured values are very close to the ideal ones and this happens mainly due to the symmetry of the structure.

In references [15] and [21] the technology used offers the advantage of obtaining smaller dimensions of the circuit. Even though, the results for the electrical parameters are similar or even poorer (return loss and isolation loss in [21]) than the ones obtained for the proposed coupler. In reference [22] a coupler acting as a branch-line coupler at two frequencies (3.3 GHz and 3.85 GHz) and as a rat-race coupler at 5.3 GHz is proposed. The technology used is microstrip and the dimensions are comparable to the ones of the coupler in this paper. The return and isolation losses are 18.5 dB and 20 dB for the rat-race coupler behavior rather than 33.64 dB and 38.8 dB as in the case of the proposed coupler. Also, the phase imbalance is not so good, being around 4° rather than only 1° as in the case of the proposed coupler. The coupler presented in reference [23] has good results for the main electrical parameters, except for the return loss, but the dimensions of the overall circuit are two times greater than in the case of the proposed coupler.

Analyzing the results synthesized in Table 6 for the return loss, the performances are slightly better for the first frequency than for the second one. The rest of the parameters have similar performances for both frequencies.

Comparing the results with the ones from literature, in [2], [3], [5], [15], [21]–[23] the proposed coupler offers better performances for almost all parameters at the central frequencies.

The next step for a better comparison of coupler's performances is to compute the relative bandwidth, expressed in percentage, which is related to the central frequency of the two working bands. A threshold of 15 dB for the return loss and isolation loss is imposed. A relative bandwidth of 22.7 % (0.99-1.24 GHz) for the return loss at 1.1 GHz, respectively 18.4 % (2.3-2.76 GHz) at 2.5 GHz is measured. In the case of the isolation loss, the relative bandwidth is 20 % (1.01-1.23 GHz) for the first frequency, respectively 18.8 %

TABLE 7. Compared results between the proposed dual band ring coupler and similar hybrid couplers in literature.

Parameters	Proposed	[2]	[3]	[5]	[15]	[21]	[22]	[23]
Technology	Microstrip and lumped elements	Microstrip and lumped elements	Microstrip	Microstrip and lumped elements	Silicon based integrated passive device	Integrated passive device (IPD)	Microstrip	Microstrip and CMOS switches
Frequency [GHz] f_1/f_2	1.1 / 2.5	2.4/ 5.2	0.88/ 1.98	1.5/ 2.5	2.45/ 5.5	1.5/ 2.5	3.3&3.85/ 5.3	0.9/1.7
Frequency ratio	2.272	2.166	2.25	1.666	2.24	1.666	1.6&1.376	1.888
Coupling level [dB]	3/3	3/3	3/3	3/3	3/0	3/3	3/3	3/3
Type of coupler	ring/ ring	ring/ ring	ring/ ring	branch-line/ ring	ring/ ring	branch-line/ ring	branch-line/ ring	ring/ring
Return loss [dB]	41/ 33.64	19.62/ 23.39	39/ 28.5	22/ 22	20.8/19.8	20/ 24	10.5&21.5/ 18.5	10/15
Isolation loss [dB]	33.14/ 38.8	29.97/ 22.11	40.3/ 29.5	16.5/ 40	38.2/22.3	14/ 29.5	18&24/20	26/30
Insertion loss [dB]	3.47/ 3.52	4.04/ 4.09	3.3/ 3.3	4.3/ 3.7	2.78/ 4.72	6.9/ 5	4.8&3/5	3.9/4.3
Coupling loss [dB]	3.44/ 3.57	3.83/ 4.53	3/ 3.7	4.6/ 3.9	5.73/ 4.38	5.7/ 4.3	3&3.6/5	3.9/4.3
Output phase difference – ang(S_{21})-ang(S_{41}) [deg]	181.1/ -181.4	N.A./ N.A.	184.6/ 177.8	93.2/ 188.9	183.5/ 182	~90/ ~180	88&89/176	~183/~179
Output phase difference – ang(S_{12})-ang(S_{32}) [deg]	1.18/ -1.04	4.3/ 1.9	5.1/ 4.9	N.A./ 5.5	0.05/ 0.75	N.A./ ~0	N.A./3.7	N.A./N.A.
Circuit Area (mm^2)	11 × 13	22.52 × 22.52	N.A.	~22.5 × 39.2	4.35 × 3.1	7.15 × 5.15	13.8 × 11.3	~35 × 35

(2.29-2.76 GHz) for the second frequency. For the insertion loss and coupling loss a 1.5 dB imbalance is imposed and a relative bandwidth of 17.27 % (0.99-1.18 GHz) for the first frequency, respectively 18.8 % (2.38-2.85 GHz) for the second frequency is obtained. The bandwidth for the phase difference by imposing an imbalance of 10° is 18.18 % (1.02-1.22 GHz) for the first frequency and 17.2 % (2.32-2.75 GHz) for the second one. Using the same limitations for the electrical parameters, in the ideal case, as shown in Fig. 18 and 19, the relative bandwidth for both frequency bands does not exceed 25%. Comparing these results with a classical ring coupler, we can see that it remains a narrow band device, but which can be used with similar performances at two arbitrary frequencies. Another important aspect is that this novel ring coupler is miniaturized by using only one cell for each metamaterial transmission line.

In [5] a fractional bandwidth of 16 % is reported at 2.5 GHz, which is smaller than the ones measured in this paper, but comparable. This happens mainly because the authors in [5] use the same technology and the limitations imposed by a lumped elements' design are identical.

So, it can be concluded that coupler proposed in this paper can work with similar performances for both frequencies, its dimensions have been reduced and the implementation can be done easily by applying the principle of LH TLs' duality.

It can be used to realize pattern diversity in Multiple Input Multiple Output (MIMO) systems and it can act as a decoupling network in the receiver. Another industrial application of this coupler is the fact that it can be used for different standards, using different frequencies, having similar performances and a cost reduction.

V. CONCLUSION

In this paper a miniaturized 3-dB dual band ring coupler with metamaterial impedance inverters transmission lines is proposed and tested. It is designed to work at two arbitrary frequencies, 1.1 GHz and 2.5 GHz, with similar performances. The dualism of the CRLH and D-CRLH transmission lines' characteristics is investigated in detail, offering the possibility to design ring couplers with very good performances, for any arbitrary coupling levels (except for 0-dB). The design of the miniaturized CRLH/D-CRLH

impedance inverter lines assures a minimum number of cells and consequently less components. The 3-dB coupler has a dimension of $0.07\lambda \times 0.07\lambda$, with λ computed at 1.1 GHz, which demonstrates its compactness. The performances are similar for both frequencies, having a return loss and isolation better than 33 dB and an insertion and coupling loss at around 3.5 dB for both frequency bands. The output phase difference is around $\pm 181^\circ$ for both frequencies, when the difference port is excited and is around $\pm 1^\circ$, when the sum ports is excited. The relative bandwidth is similar for all parameters. One way of improving the bandwidth is to avoid using lumped elements and to use an odd number of impedance inverter unit cells. This type of coupler can be redesigned successfully for any other frequencies and coupling levels, except for 0-dB.

ACKNOWLEDGMENT

The author wants to thank Ph.D. Eng. G. I. Sajin for all the support.

REFERENCES

[1] C. Y. Pon, "Hybrid-ring directional coupler for arbitrary power divisions," *IEEE Trans. Microw. Theory Techn.*, vol. MTT-9, no. 6, pp. 529–535, Nov. 1961, doi: 10.1109/TMTT.1961.1125385.

[2] P.-L. Chi, C.-J. Lee, and T. Itoh, "A compact dual-mand metamaterial-based rat-race coupler for a MIMO system application," in *IEEE MTT-S Int. Microw. Symp. Dig.*, Jun. 2008, pp. 667–670, doi: 10.1109/MWSYM.2008.4632920.

[3] K.-K.-M. Cheng and F.-L. Wong, "A novel rat race coupler design for dual-band applications," *IEEE Microw. Wireless Compon. Lett.*, vol. 15, no. 8, pp. 521–523, Aug. 2005, doi: 10.1109/LMWC.2005.852792.

[4] P. Chi and P. Huang, "Miniaturized dual-band ring coupler with arbitrary power divisions using composite right/left-handed transmission lines," in *Proc. Asia–Pacific Microw. Conf.*, Nov. 2014, pp. 19–21.

[5] L. Chang and T.-G. Ma, "Dual-mode branch-line/rat-race coupler using composite right-/left-handed lines," *IEEE Microw. Wireless Compon. Lett.*, vol. 27, no. 5, pp. 449–451, May 2017, doi: 10.1109/LMWC.2017.2690851.

[6] H.-R. Ahn and M. M. Tentzeris, "Compact and wideband general coupled-line ring hybrids (GCRHs) for arbitrary circumferences and arbitrary power-division ratios," *IEEE Access*, vol. 7, pp. 33414–33423, 2019, doi: 10.1109/ACCESS.2019.2902852.

[7] G. Siso, J. Bonache, and F. Martin, "Dual-band rat race hybrid coupler implemented through artificial lines based on complementary split ring resonators," in *IEEE MTT-S Int. Microw. Symp. Dig.*, Boston, MA, USA, Jun. 2009, pp. 625–628.

[8] T. Djerafi, H. Aubert, and K. Wu, "Ridge substrate integrated waveguide (RSIW) dual-band hybrid ring coupler," *IEEE Microw. Wireless Compon. Lett.*, vol. 22, no. 2, pp. 70–72, Feb. 2012.

[9] Y. Dong and T. Itoh, "Application of composite right/left-handed half-mode substrate integrated waveguide to the design of a dual-band rat-race coupler," in *IEEE MTT-S Int. Microw. Symp. Dig.*, Anaheim, CA, USA, May 2010, pp. 712–715.

[10] L.-S. Wu, J. Mao, and W. Y. Yin, "Miniaturization of rat-race coupler with dual-band arbitrary power divisions based on stepped-impedance double-sided parallel-strip line," *IEEE Trans. Compon., Packag., Manuf. Technol.*, vol. 2, no. 12, pp. 2017–2030, Dec. 2012.

[11] C.-L. Hsu, C.-W. Chang, and J.-T.Kuo, "Design of dual-band microstrip rat race coupler with circuit miniaturization," in *IEEE MTT-S Int. Microw. Symp. Dig.*, Jun. 2007, pp. 177–180, doi: 10.1109/MWSYM.2007.380319.

[12] T. Kawai, Y. Tanabe, A. Enokihara, and I. Ohta, "Compact dual-band rat-race hybrid utilizing composite right/left-handed transmission lines," in *Proc. 41st Eur. Microw. Conf.*, Oct. 2011, pp. 285–288, doi: 10.23919/EuMC.2011.6101946.

[13] M.-L. Chuang, "Miniaturized ring coupler of arbitrary reduced size," *IEEE Microw. Wireless Compon. Lett.*, vol. 15, no. 1, pp. 16–18, Jan. 2005.

[14] C.-H. Tseng, C.-H. Mou, C.-C. Lin, and C.-H. Chao, "Design of microwave dual-band rat-race couplers in printed-circuit board and GIPD technologies," *IEEE Trans. Compon., Packag., Manuf. Technol.*, vol. 6, no. 2, pp. 262–271, Feb. 2016, doi: 10.1109/TCPMT.2015.2507371.

[15] Y.-S. Lin, Y.-R. Liu, and C.-H. Chan, "Novel miniature dual-band rat-race coupler with arbitrary power division ratios using differential bridged-T coils," *IEEE Trans. Microw. Theory Techn.*, vol. 69, no. 1, pp. 590–602, Jan. 2021, doi: 10.1109/TMTT.2020.3035287.

[16] A. Sanada, C. Caloz, and T. Itoh, "Characteristics of the composite right/left-handed transmission lines," *IEEE Microw. Wireless Compon. Lett.*, vol. 14, no. 2, pp. 68–70, Feb. 2004, doi: 10.1109/LMWC.2003.822563.

[17] C. Caloz, "Dual composite right/left-handed (D-CRLH) transmission line metamaterial," *IEEE Microw. Wireless Compon. Lett.*, vol. 16, no. 11, pp. 585–587, Nov. 2006, doi: 10.1109/LMWC.2006.884773.

[18] I. A. Mocanu and T. Petrescu, "Novel dual band hybrid rat-race coupler with CRLH and D-CRLH transmission lines," in *Proc. Asia–Pacific Microw. Conf.*, Dec. 2011, pp. 888–891.

[19] I. A. Mocanu, "Dual band rat race coupler for 4G applications using CRLH and D-CRLH transmission lines," in *Proc. 18th Int. Conf. Commun. (CSCC)*, 2014, pp. 80–86.

[20] I. Mocanu, "The influence of cell symmetry in the performances of DCRLH branch line couplers," *UPB Sci. Bull. C*, vol. 74, no. 2, pp. 157–166, 2012.

[21] H. N. Chu, G.-Y. Li, and T.-G. Ma, "Dual-mode coupler with branch-line/rat-race responses on integrated passive device process," in *IEEE MTT-S Int. Microw. Symp. Dig.*, Jul. 2019, pp. 82–84, doi: 10.1109/IMWS-AMP.2019.8880088.

[22] M. S. Ghaffarian, G. Moradi, and P. Mousavi, "Dual band/ dual mode branch-line/rat-race coupler using artificial transmission line," in *Proc. 27th Iranian Conf. Electr. Eng. (ICEE)*, Apr. 2019, pp. 1622–1626, doi: 10.1109/IranianCEE.2019.8786478.

[23] E. Tolin, A. Bahr, and F. Vipiana, "Miniaturized and reconfigurable rat-race coupler based on artificial transmission lines," *IEEE Microw. Wireless Compon. Lett.*, vol. 30, no. 4, pp. 375–378, Apr. 2020, doi: 10.1109/LMWC.2020.2972738.

IULIA ANDREEA MOCANU was born in Craiova, Romania. She received the B.Sc. and the Ph.D. degrees in electronics and electrical engineering from the University Politehnica of Bucharest (UPB), Bucharest, in 2007 and 2011, respectively.

Since 2007, she has been with the Department of Telecommunications, UPB. From 2012 to 2013, she was a Researcher with the Microwave Group, National Institute for Research and Development in Microtechnologies-IMT Bucharest, where she was involved with metamaterial microstrip and coplanar microwave circuit designs. From 2013 to 2014, she was a Postdoctoral Researcher with the University Politehnica of Bucharest, where she studied artificial transmission lines and their applications for innovative microwave circuits. Her current research interests include higher-order symmetry, microwave circuits, artificial LH transmission lines, and electromagnetic propagation.